OXFORD

SOT | Society of Toxicology
academic.oup.com/toxsci

TOXICOLOGICAL SCIENCES, 2020, 1–11

doi: 10.1093/toxsci/kfaa158
Dryad Digital Repository DOI: https://doi.org/10.5061/dryad.h18931zj8
Advance Access Publication Date: 16 October 2020
Research Article

PCB126 Exposure Revealed Alterations in m6A RNA Modifications in Transcripts Associated With AHR Activation

Neelakanteswar Aluru[1] and Sibel I. Karchner

Biology Department and Woods Hole Center for Oceans and Human Health, Woods Hole Oceanographic Institution, Woods Hole, Massachusetts 02543

[1]To whom correspondence should be addressed at Biology Department, MS-32, Woods Hole Oceanographic Institution, Woods Hole, MA 02543. E-mail: naluru@whoi.edu.

ABSTRACT

Chemical modifications of proteins, DNA, and RNA moieties play critical roles in regulating gene expression. Emerging evidence suggests the RNA modifications (epitranscriptomics) have substantive roles in basic biological processes. One of the most common modifications in mRNA and noncoding RNAs is N^6-methyladenosine (m6A). In a subset of mRNAs, m6A sites are preferentially enriched near stop codons, in 3′ UTRs, and within exons, suggesting an important role in the regulation of mRNA processing and function including alternative splicing and gene expression. Very little is known about the effect of environmental chemical exposure on m6A modifications. As many of the commonly occurring environmental contaminants alter gene expression profiles and have detrimental effects on physiological processes, it is important to understand the effects of exposure on this important layer of gene regulation. Hence, the objective of this study was to characterize the acute effects of developmental exposure to PCB126, an environmentally relevant dioxin-like PCB, on m6A methylation patterns. We exposed zebrafish embryos to PCB126 for 6 h starting from 72 h post fertilization and profiled m6A RNA using methylated RNA immunoprecipitation followed by sequencing (MeRIP-seq). Our analysis revealed 117 and 217 m6A peaks in the DMSO and PCB126 samples (false discovery rate 5%), respectively. The majority of the peaks were preferentially located around the 3′ UTR and stop codons. Statistical analysis revealed 15 m6A marked transcripts to be differentially methylated by PCB126 exposure. These include transcripts that are known to be activated by AHR agonists (eg, *ahrra*, *tiparp*, *nfe2l2b*) as well as others that are important for normal development (*vgf, cebpd, sned1*). These results suggest that environmental chemicals such as dioxin-like PCBs could affect developmental gene expression patterns by altering m6A levels. Further studies are necessary to understand the functional consequences of exposure-associated alterations in m6A levels.

Key words: dioxin-like PCBs; development; zebrafish; epitranscriptomics; m6A; MeRIP.

Epigenetic regulation of gene expression has been shown to play critical roles in basic biological processes in vertebrates. Enormous strides have been made in our understanding about the role of DNA methylation and chromatin modifications in gene regulation. Recent studies have demonstrated another layer of epigenetic regulation at the RNA level, where internal chemical modifications of mRNA have been shown to affect their stability, processing, localization, and splicing. There are over 160 different RNA modifications that have been identified and their roles in embryonic development, nervous system function, and multigenerational effects have been demonstrated.

One of the most common modifications in mRNA and non-coding RNAs is N^6-methyladenosine (m6A). In a subset of

mammalian mRNAs, m6A sites are preferentially enriched near stop codons, in 3′ UTRs, and within long internal exons with a consensus sequence of RRACH (R = G or A; H = A, C or U), suggesting an important role in the regulation of gene expression. m6A has been shown to regulate RNA processing, including RNA splicing (Kasowitz *et al.*, 2018; Tang *et al.*, 2018), nuclear export (Roundtree *et al.*, 2017), RNA degradation (Zheng et al., 2013), and translation (Huang *et al.*, 2018; Shi *et al.*, 2017). The enzymatic machinery involved in writing, reading, and removing the m6A modifications have been identified. A multicomponent writer complex consisting of the catalytic subunit methyltransferase like 3 (METTL3) is responsible for m6A RNA methylation, whereas fat mass and obesity-associated protein (FTO) and α-ketoglutarate-dependent dioxygenase alkB homolog 5 (ALKBH5) have been identified as the m6A erasers (Meyer and Jaffrey, 2017). Additionally, m6A can be recognized by multiple RNA-binding proteins, such as the YTH domain family proteins and the heterogeneous nuclear ribonucleoprotein (HNRNP) family (Meyer and Jaffrey, 2017; Roundtree *et al.*, 2017; Zhou *et al.*, 2019). Gene deletion studies have revealed that loss of *mettl3* in mice is embryonic lethal and leads to complete loss of m6A in polyadenylated RNA (Geula *et al.*, 2015). In contrast, *fto* knockout mice develop normally and show elevated m6A levels selectively in the 5′ UTR (Jia *et al.*, 2011) but recent results suggests that *fto* non-specifically targets m6A (Mauer and Jaffrey, 2018; Zaccara *et al.*, 2019). In addition, deletion of a YTH domain containing protein, *ythdf2* has been shown to increase the half-lives of mRNAs compared with those lacking m6A (Zhao *et al.*, 2017). These studies demonstrate that m6A RNA methylation is under the regulation of these three important group of proteins. There is growing evidence that these proteins play an important role in a number of physiological processes including stress response (Batista *et al.*, 2014; Chen *et al.*, 2015; Engel *et al.*, 2018; Fischer *et al.*, 2009; Schwartz *et al.*, 2014; Zhang *et al.*, 2017; Zhao *et al.*, 2017). However, there is very limited information about the impact of environmental chemicals on m6A methylation patterns and the associated functional consequences on gene expression patterns (Cayir *et al.*, 2020). Recent studies have demonstrated that environmental chemicals such as arsenite affect m6A RNA methylase and demethylase protein expression (Bai *et al.*, 2018; Cayir *et al.*, 2019; Chen *et al.*, 2019; Gu *et al.*, 2018; Zhao *et al.*, 2019). These studies have also measured global m6A RNA content using an ELISA-based method. However, this approach does not provide any information about the location of the m6A modifications.

Even though the existence of m6A RNA modification has been known for a long time (Desrosiers *et al.*, 1974), recent advances in the transcriptome-wide m6A quantification methods (Dominissini *et al.*, 2013; Linder *et al.*, 2015; Meyer *et al.*, 2012) have yielded unprecedented insights into the location of m6A in RNAs. To date, majority of the studies have relied on immunoprecipitation of methylated RNAs using m6A-recognizing antibodies such as methylated RNA immunoprecipitation followed by sequencing (MeRIP-seq) (Meyer *et al.*, 2012). Using MeRIP-seq, we tested the hypothesis that developmental exposure to environmental chemicals causes alterations in m6A RNA methylation patterns.

The objective of this study was to characterize the acute effects of developmental exposure to PCB126, an environmentally relevant dioxin-like PCB, on m6A methylation patterns. The experiments reported here were conducted in zebrafish, a well-established and widely used model for developmental toxicology (Behl *et al.*, 2019; Nishimura *et al.*, 2016) and human diseases (Bradford *et al.*, 2017; Grunwald and Eisen, 2002). Zebrafish embryos were exposed to PCB126 for 6 h starting from 72 h post fertilization (hpf) and profiled m6A RNA using MeRIP-seq, as well as assessing changes in mRNA expression and splicing. As many of the commonly occurring environmental contaminants alter gene expression profiles and have detrimental effects on physiological processes, it is important to understand the effects of exposure on this important layer of gene regulation.

MATERIALS AND METHODS

Experimental Animals

The wild-type AB strain of zebrafish was used in this study. All experiments were conducted as per protocols approved by the Animal Care and Use Committee of the Woods Hole Oceanographic Institution. Freshly fertilized eggs were obtained from breeding of multiple tanks with 20–25 male and female fish.

Developmental Exposure to PCB126

Zebrafish embryos were exposed to 10 nM PCB126 (3,3',4,4',5-pentachlorobiphenyl, 99.2% purity; UltraScientific, Rhode Island) or DMSO (solvent control; 0.01%) starting at 72 hpf for 6 h. This concentration and duration of exposure was chosen based on previous observations that this regime causes AHR activation in zebrafish embryos (Jonsson *et al.*, 2012). These concentrations are found in highly contaminated environments such as the New Bedford Harbor Superfund site (Nacci *et al.*, 2010). According to NHANES data, both dioxin-like and non-dioxin-like PCBs are found in human blood samples at nanogram levels (Faroon and Ruiz, 2016; Yang *et al.*, 2018). Each treatment consisted of 4 biological replicates with 48 embryos per replicate. Embryos were maintained in glass petri dishes at 28 ± 0.5°C at a density of 1 embryo per ml in 0.3X Danieau's solution (pH 7.2). At the end of the exposure, embryos were thoroughly rinsed with 0.3X Danieau's solution and sampled for MeRIP sequencing.

Total RNA Isolation

DNase-free total RNA was isolated using the BioRad Aurum kit following manufacturer's instructions. Quantity and quality of total RNA was determined using the Qubit RNA high sensitivity assay kit (Thermo Fisher Scientific) and Agilent Bioanalyzer, respectively. All samples had an RNA integrity number above 9.3.

MeRIP Sequencing

m6A RNA was immunoprecipitated with an anti-m6A antibody (rabbit polyclonal; Synaptic Systems, Germany; catalog no. 202 003; RRID: AB_2279214). This antibody has been extensively used for m6A RNA immunoprecipitation (Dominissini *et al.*, 2013; Engel *et al.*, 2018; Zeng *et al.* 2018; Zhong *et al.* 2018), including zebrafish (Zhao *et al.*, 2017). MeRIP-seq was conducted following a recently published protocol using low quantities of total RNA (Zeng *et al.*, 2018). Briefly, the protocol involves RNA fragmentation, m6A immunoprecipitation, and sequencing library preparation. For each sample, 18 μg of total RNA was chemically fragmented in 20 μl volume with the RNA fragmentation reagent at 70°C (Thermo Fisher Scientific Inc.). The fragmentation reaction was stopped by adding a stop solution and precipitated overnight at −80°C with 3 M sodium acetate, glycogen, and 100% ethanol. The precipitated RNA was pelleted by centrifugation, washed with 75% ethanol and resuspended in molecular-grade water. The size distribution of fragmented RNA was assessed using the Bioanalyzer.

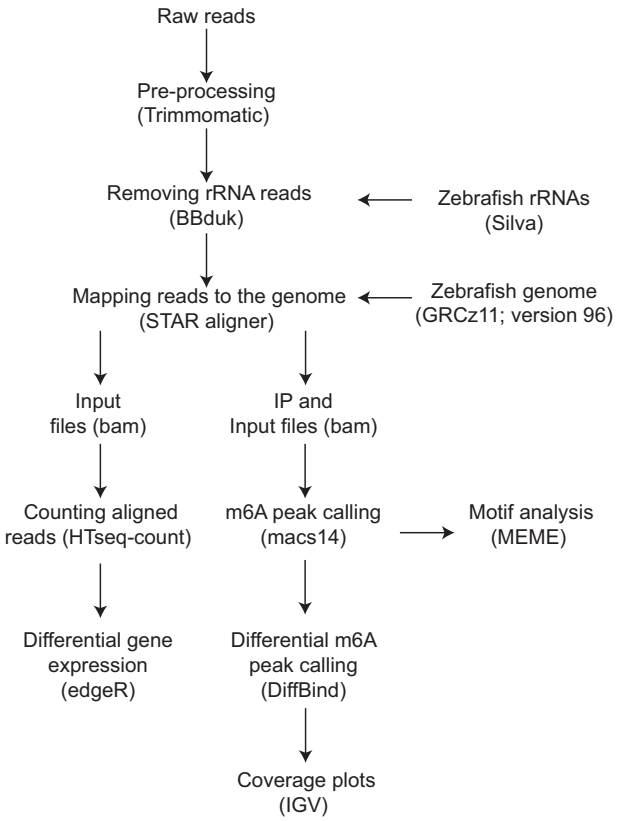

Figure 1. Overview of the MeRIP analysis pipeline. Raw reads were trimmed and ribosomal RNA reads were filtered prior to mapping to the genome and m6A peak calling, followed by statistical analysis. Integrated Genome Viewer (IGV) was used to visualize the m6A peaks. Input reads were used for differential gene expression and exon usage analysis. The detailed description of the analysis is provided in the Materials and Methods section.

m6A RNA was immunoprecipitated by incubating the fragmented RNA with 5 μg of anti-m6A antibody-magnetic bead mixture. This mixture was prepared by incubating the antibody with 30 μl each of protein A and G magnetic beads in immunoprecipitation buffer for at least 6 h at 4°C. The antibody-bead mixture was washed with IP buffer and incubated with fragmented RNA for 2 h at 4°C. RNasin Plus RNase inhibitor was added to the incubation mix to prevent RNA degradation. Following incubation, the antibody-bead mixture was washed twice with IP buffer, followed by low and high salt buffers for 10 min each at 4°C. The m6A-enriched fragmented RNA was eluted from the beads and purified using the RNeasy mini kit (Qiagen). The quality of the m6A-enriched RNA was assessed with the Bioanalyzer. m6A and input RNA libraries were prepared using the SMARTer stranded total RNA-seq kit (Clontech) and sequenced on the Illumina NextSeq500 platform (75 bp, paired end reads) at the Tufts university sequencing core facility.

MeRIP-Seq Data Analysis

Mapping. Data analysis (Figure 1) was carried out following previously established protocols for analysis of genome-wide m6A patterns (Dominissini *et al.*, 2013). Raw reads from individual samples were pre-processed using Trimmomatic to remove adapters and low quality reads. Ribosomal reads were removed from downstream processing by mapping the pre-processed

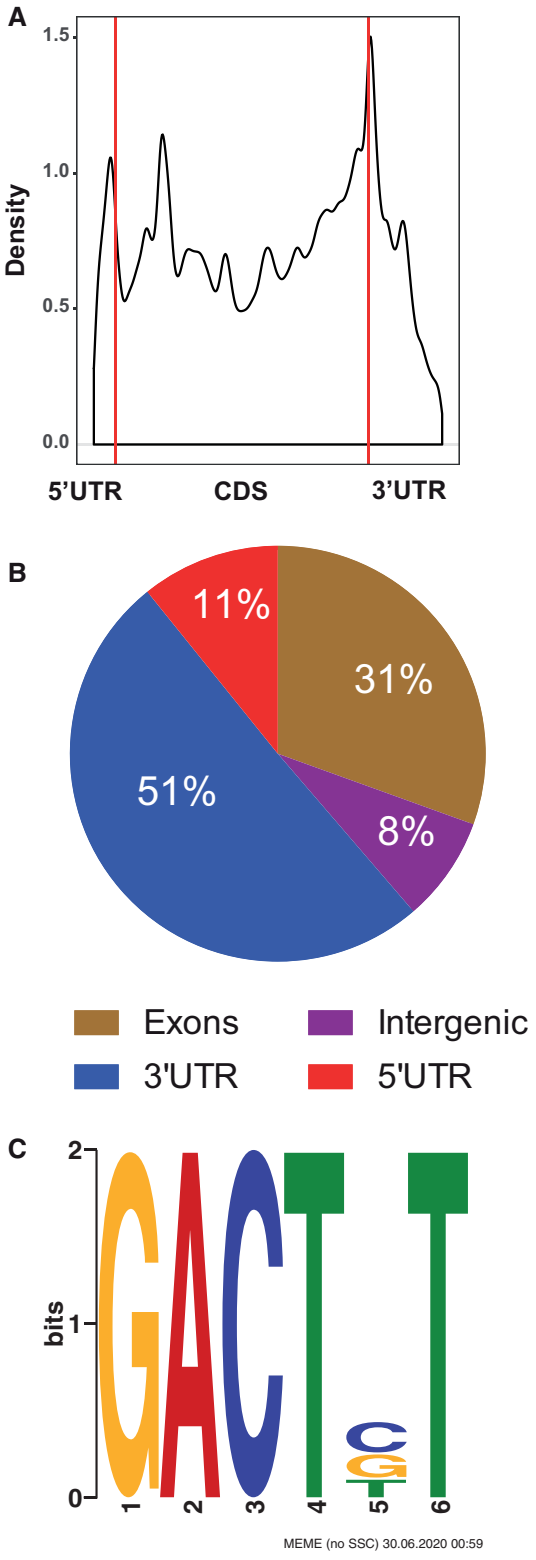

Figure 2. m6A RNA methylation landscape in zebrafish embryos. A, Metagene profiles of m6A distribution across the transcriptome in control samples. B, Distribution of m6A peaks in the different transcript regions (5′ and 3′ UTR, exons and introns). C, Consensus sequence motif for m6A RNA methylation identified in control samples.

A

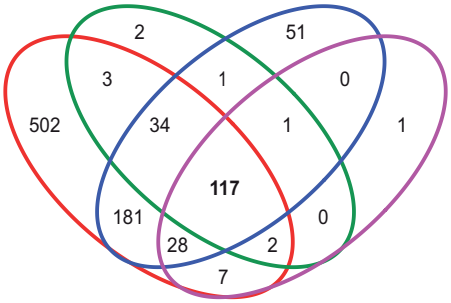

B

Term ID	Term name	Adjusted p.value
Molecular Function		
GO:0008327	Methyl CpG binding	7.16E-09
GO:0000384	Spliceosomal transesterification activity	4.98E-06
Biological Process		
GO:0007399	Nervous system development	1.85E-09
GO:0000381	Regulation of alternative mRNA splicing via spliceosome	4.20E-05
GO:0006278	RNA-dependent DNA biosynthetic process	4.47E-04

C

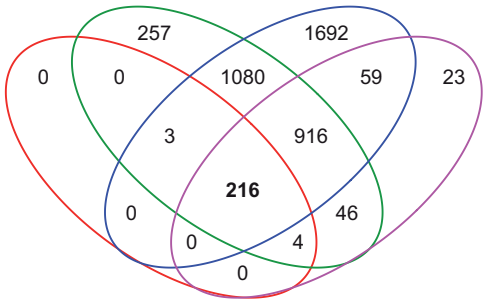

D

Term ID	Term name	Adjusted p.value
Molecular Function		
GO:0003723	RNA binding	1.51E-07
GO:0016886	Ligase activity, forming phosphoric ester bonds	2.11E-05
GO:0000384	First spliceosomal transesterification activity	3.70E-03
Biological Process		
GO:0071897	DNA biosynthetic process	4.79E-05
GO:1903311	Regulation of mRNA metabolic process	1.03E-03
GO:0070198	Protein localization to chromosome, telomeric region	1.04E-04
GO:0043484	Regulation of RNA splicing	1.01E-04
GO:0031175	Neuron projection development	1.01E-03

Figure 3. m6A RNA modification patterns in DMSO and PCB126 samples. A and C, Venn diagram showing the unique and shared m6A peaks among biological replicates in DMSO and PCB126 groups. B and D, Gene Ontology analysis (Biological Process and Molecular Function) of m6A peaks common to all 4 biological replicates in DMSO and PCB126.

reads to the ribosomal sequences. The zebrafish ribosomal sequences were downloaded from the Silva database (https://www.arb-silva.de/). Ribosomal-free reads were mapped to the zebrafish genome (GRCz11 version 96) using the STAR aligner version 2.6.0d (Dobin *et al.*, 2013). The resulting unique reads were used for peak calling.

Peak calling and visualization. We used Model-based Analysis of ChIP-Seq (MACS) algorithm (version 1.4.2) for identification of the m6A peaks. The immunoprecipitated (m6A) and input (fragmented RNA) samples were used as treatment and control input files, respectively. The effective genome size (–gsize) was set to 117,608,789. The coverage data (wiggle files) was normalized to obtain comparable read density between input and IP samples and visualized using the UCSC genome browser.

Motif search and peak annotation. *De novo* motif finding was done using MEME (Bailey *et al.*, 2009). The FASTA file of the 50-bp region flanking the peak summits was used as input and the top 3 consensus motifs were retrieved. CentriMO (Bailey and Machanick, 2012) was used for visualization of the positional distribution of the best match of the m6A motif in the 300 bp centered around the peak summits.

Statistical analysis. Differential methylation analysis was done following the guidelines recommended for MeRIP analysis (McIntyre *et al.*, 2020). We used DiffBind, a bioconductor package, for differential m6A peak calling (Stark and Brown, 2011).

Gene Expression Profiling

The input RNA samples were used for differential gene expression analysis. The number of reads mapped to the annotated regions of the genome was obtained with HTSeq-count (Anders *et al.*, 2015). Statistical analysis was conducted using edgeR, a Bioconductor package (Robinson *et al.*, 2010). We used the quasi-likelihood model in edgeR (glmQLFTest) to perform differential gene expression analysis. Only genes with a false discovery rate (FDR) of less than 5% were considered to be differentially expressed. Annotation of the differentially expressed genes (DEGs) was done using BioMart (Smedley *et al.*, 2015).

Differential Exon Usage Analysis

To obtain the differentially used exons (DUEs), we used DEXSeq (Anders *et al.*, 2012) and compared the exon usage between DMSO and PCB126 exposed groups in input RNA samples. DUEs are defined as a change in exon usage where exon usage is defined as the ratio of reads mapping to a particular exon versus reads mapping anywhere else in a gene (Anders *et al.*, 2012). RNAseq data from the input samples were used for estimating DUEs. We considered exons to be differentially used when their adjusted *p*-value was below .05 (Benjamini Hochberg correction).

RESULTS

All the raw and processed data from this study have been deposited into Gene Expression Omnibus (accession number GSE153436) and Dryad (Aluru and Karchner, 2020).

m6A Methylation Profiles in Zebrafish

MeRIP-sequencing of zebrafish embryos revealed highly conserved characteristics of m6A RNA methylation. For instance, m6A RNA methylation is predominantly found in the 3′ UTR. The metagene plot of a subset of the m6A peaks shows the characteristic peak in RNA methylation around the end of the coding sequence and beginning of the 3′ UTR (Figure 2A). The pie chart representation of all the m6A peaks shows that 51% of the peaks are found in the 3′ UTR (Figure 2B). Motif search of the m6A peaks identified previously established RRACH consensus sequence observed in vertebrates (*E*-value = 5.2E–35; Figure 2C).

The number of m6A peaks among the DMSO replicates range from 156 to 875 (FDR 5%). Among them, 117 peaks were common to all biological replicates (Figure 3A). Gene ontology (GO) term analysis of the common peaks revealed enrichment of biological process terms—nervous system development (GO: 0007399), regulation of alternative mRNA splicing via spliceosome (GO: 0000381) and RNA-dependent DNA biosynthetic process (GO: 0006278), and molecular function terms—methyl CpG binding (GO: 0008327) and first spliceosomal transesterification activity (GO: 0000384) (Figure 3B).

Similarly, the number of m6A peaks among the PCB replicates range from 224 to 3971 (FDR 5%). Among them, 217 peaks were common to all biological replicates (Figure 3C). GO term analysis of the common peaks revealed enrichment of biological process terms—DNA biosynthetic process (GO: 0071897), regulation of mRNA metabolic process (GO: 1903311), protein localization to chromosome, telomeric region (GO: 0070198), regulation of RNA splicing (GO:0043484) and neuron projection development (GO: 0031175), and molecular function terms—RNA binding (GO: 0003727), ligase activity (GO: 0016886), and first spliceosomal transesterification activity (GO: 0000384) (Figure 3D).

PCB126 Exposure Induced Changes in m6A RNA Methylation

Principal component analysis (PCA) revealed one of the treatment biological replicates as an outlier (Supplementary Figure S1). We omitted this replicate from statistical analysis. Based on the comparison between peaks that were present in both PCB126 (3 replicates) and DMSO (4 biological replicates) samples, we observed 15 differentially methylated peaks (DESeq2, 5%FDR), and 11 of these showed higher methylation in response to PCB126 (Figure 4A). The genomic coordinates, read counts, and the statistical significance of the differentially methylated peaks are provided in Supplementary Table S1. The complete list of all the m6A methylated peaks is provided in Supplementary Material (Differential_m6A_methylation_DiffBind.xlsx). These peaks include aryl hydrocarbon receptor repressor a (*ahrra*), TCDD-inducible poly(ADP-ribose) polymerase (*tiparp*), pleckstrin homology, MyTH4 and FERM domain-containing H3 (*plekhh3*), nuclear factor, erythroid 2-like 2b (*nfe2l2b*), protein phosphatase 1 regulatory subunit 18 (*ppp1r18*), retinitis pigmentosa GTPase regulator a (*rpgra*), znf648, pleckstrin homology domain-containing family G member 4B (*plekhg4b*, si: dkey-65j6.2), FP236157.6 (lincRNA), collagen-type XXIV alpha 1 chain (*col24a1;* CABZ01071903.1), and one unannotated region. Four differentially methylated peaks were reduced in response to PCB126 exposure and these include VGF nerve growth factor inducible (*vgf*), CCAAT enhancer binding protein delta (*cebpd*), si: dkey-175g6.2 (orthologous to human VGF) and *sushi, nidogen, and EGF-like domains 1* (*sned1*). Representative m6A peak coverage plots from *ahrra* (Figure 4B) and *vgf* (Figure 4C) are shown as examples.

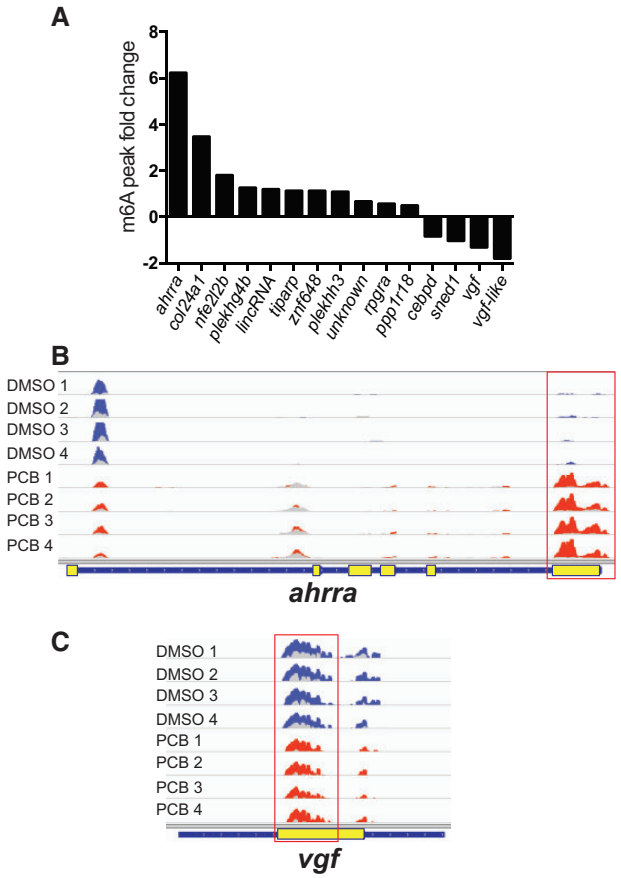

Figure 4. PCB126-induced alterations in m6A methylation patterns. A, Histogram showing the transcripts with differentially methylated m6A peaks and their fold change. B, Representative m6A peak coverage plots in DMSO and PCB126 samples. Each track is an individual biological replicate ($n = 4$). Differentially methylated m6A peak is highlighted with a red square. The input sample tracks (light color) are overlaid over the immunoprecipitated (IP) sample. DMSO and PCB126 tracks are shown in blue and red colors, respectively. Yellow boxes in the gene layout denote exons.

PCB126 Exposure Induced Differential Gene Expression and Exon Usage

RNAseq analysis of the input RNA revealed differential expression of 272 genes in response to PCB126 exposure, with 85 and 187 up and downregulated genes, respectively (Figure 5). The list of DEGs is provided in Supplementary Table S2. Complete list of results from edgeR analysis is provided in Supplementary Material (MeRIP-InputRNA-DGE.xlsx). The upregulated genes are enriched in the GO biological process term response to xenobiotic stimulus, and GO molecular function terms, such as cofactor binding, iron ion binding, intermediate filament binding, and oxidoreductase activity (Figure 5B). The upregulated genes include prototypical AHR target genes (*cyp1a*, *cyp1c1*, *cyp1c2*, *cyp1b1*, *ahrra*, *foxf2a*). The downregulated genes are enriched in GO terms such as response to peptide (biological process), organic ion transmembrane transporter activity, oxidative phosphorylation uncoupler activity, and steroid hormone receptor binding (Figure 5C). We did not observe differential expression of m6A writers, readers, and erasers. We mined the RNAseq data and tabulated their expression in the Supplementary Table S3.

Differential exon usage analysis revealed 2 transcripts (protocadherin10 and solute carrier family 66 member 1) with significant differences in exon usage. Both of these transcripts showed differential usage in 1 exon (Figure 6).

A

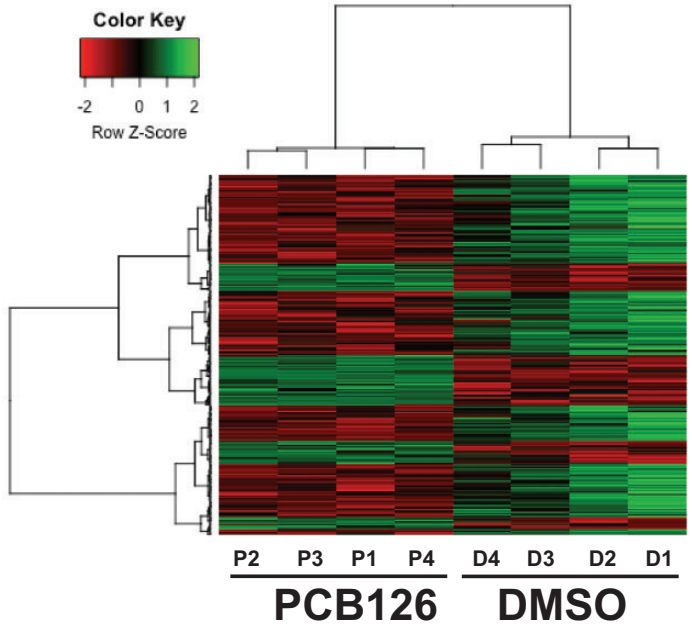

B **Upregulated genes**

Term ID	Term name	Adjusted p.value
Molecular Function		
GO:0048037	Cofactor binding	0.033
GO:00191215	Intermediate filament binding	0.02
GO:0016491	Oxidoreductase activity	0.016
GO:0005506	Iron ion binding	0.00026
Biological Process		
GO:0009410	Response to xenobiotic stimulus	1.09E-10

C **Downregulated genes**

Term ID	Term name	Adjusted p.value
Molecular Function		
GO:0008514	Organic ion transmembrane transporter activity	0.032
GO:0017077	Oxidative phosphorylation uncoupler activity	0.02
GO:0035258	Steroid hormone receptor binding	0.013
Biological Process		
GO:1901652	Response to peptide	0.03

Figure 5. PCB126-induced differential gene expression. A, Heatmap representation of the differentially expressed genes (DEGs). Differential gene expression analysis was performed on the input samples. B and C, Gene Ontology (Biological Process and Molecular Function) terms of up and downregulated DEGs and their statistical significance (adjusted p-value $< .05$).

DISCUSSION

The present study demonstrated that acute PCB126 exposure alters m6A methylation of transcripts in zebrafish embryos. The functional significance of these alterations in developmental toxicity is not yet clear. However, based on the evidence that m6A RNA methylation plays a significant role during development (Heck and Wilusz, 2019; Li *et al.*, 2019; Vu *et al.*, 2019), our results suggest that environmental chemicals can influence developmental processes by altering an important layer of post-transcriptional regulation of mRNAs and noncoding RNAs. Furthermore, m6A RNA methylation has been shown to play a key role in normal physiology and metabolism, stress response and in various types of cancer (Engel *et al.*, 2018; Galardi *et al.*, 2020; He *et al.*, 2019), suggesting additional toxicity mechanisms for environmental chemicals.

Using MeRIP-seq, an unbiased transcriptome-wide approach, we demonstrated that acute exposure to PCB126 altered m6A methylation marks in coding and noncoding RNAs. These results provide the first evidence that m6A methylation marks can be altered by environmental chemical exposures. A recent study using an ELISA-based approach have shown that environmental chemicals, such as bisphenol A, vinclozolin, sodium arsenite, and particulate matter (PM2.5) affect m6A RNA methylation levels (Cayir *et al.*, 2019). However, this approach does not show the location of the m6A alterations in the transcriptome. Using MeRIP-seq, we observed 15 transcripts to be differentially methylated in response to PCB126 exposure in zebrafish embryos. They include 11 transcripts with increased m6A methylation marks and 4 transcripts that lost methylation marks in response to PCB126 exposure. It is not clear how the gain or loss of m6A in response to PCB126 affects transcript fate,

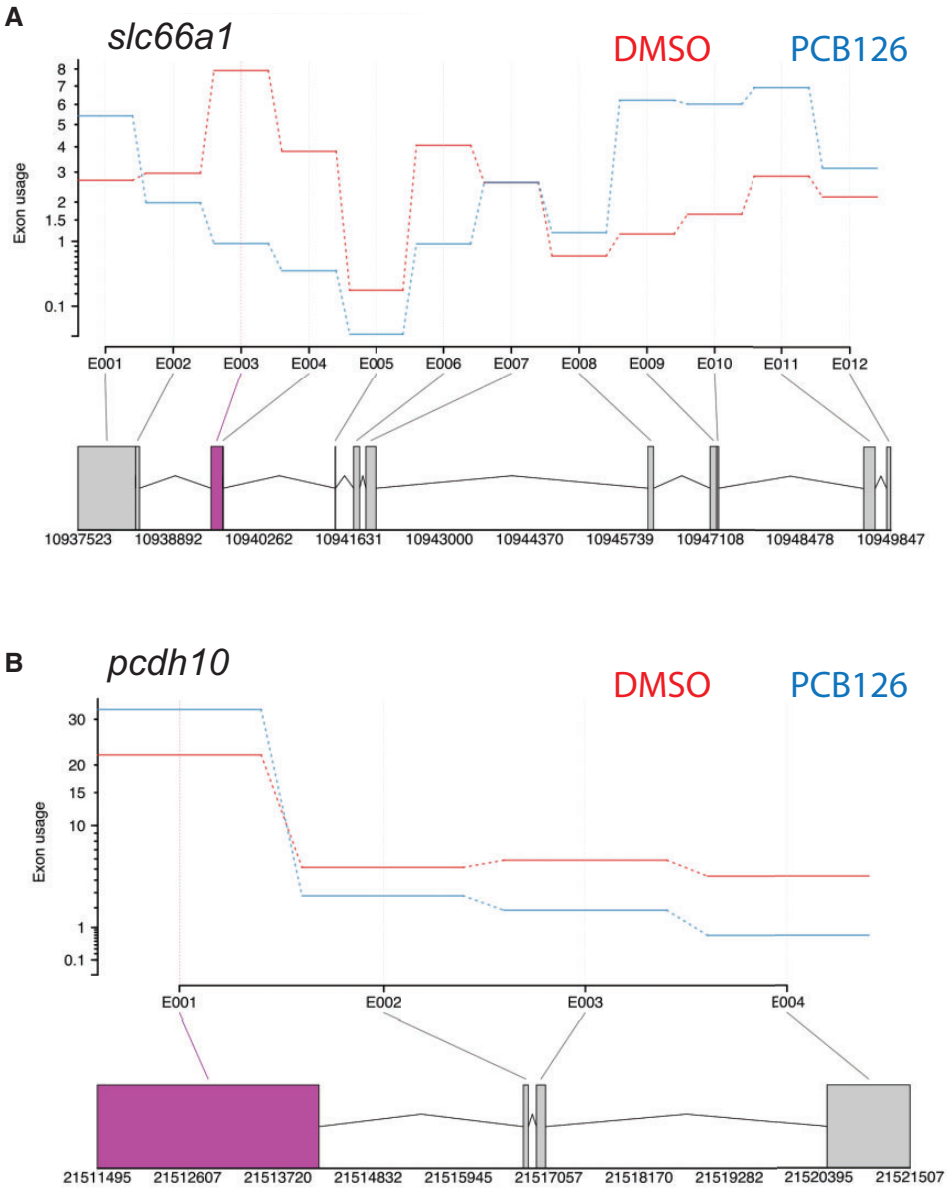

Figure 6. Effect of PCB126 exposure on differential exon usage. Gene profile plots from DEXSeq showing differential exon usage in *slc66a1* (A) and *pcdh10* (B) genes. The top panel in both figures shows changes in relative exon usage. The bottom panel shows the gene layout with different exons. The exon showing differential expression is highlighted in purple.

but recent studies have shown that m6A methylation influences RNA processing, export, translation, or decay (Coots *et al.*, 2017; Ke *et al.*, 2017; Xiao *et al.*, 2016). One of the best characterized mechanisms is the recruitment of proteins (readers) that recognize and bind to m6A modifications and how this affects RNA metabolism. One such group of m6A readers are the YTH domain containing family of proteins (eg, YTHDF1-3, YTHDC1, and YTHDC3). These proteins preferentially bind to m6A-modified RNAs, recruit other effector proteins, and influence multiple aspects of RNA metabolism (Du *et al.*, 2016; Wang *et al.*, 2015). During maternal-zygotic transition, m6A RNA methylation through recruitment of YTHDF2 has been shown to induce decay of maternal transcripts in zebrafish (Zhao *et al.*, 2017). A similar role for YTHDF2 has been observed in mammals (Ivanova *et al.*, 2017). In addition, there is compelling evidence that several other proteins such as insulin-like growth factor 2 mRNA-binding proteins (IGF2BPs) preferentially bind to m6A-modified RNAs. Further studies are needed to characterize the m6A-modified RNA-protein interactions in response to environmental chemical exposures. Surprisingly, we did not observe differential expression of any of the readers, writers, or erasers. This suggests that some of these changes might be happening in a shorter time scale and warrants time course studies.

Among the differentially methylated transcripts are products of 3 classical AHR target genes, *ahrra*, *tiparp*, and *nfe2l2b*. *Ahrr* and *tiparp* are an integral part of AHR signaling and both have been shown to negatively regulate AHR activity by distinct mechanisms (MacPherson *et al.*, 2014). In addition, recent studies demonstrated that *nrf2b*, a homolog of mammalian nuclear factor, erythroid 2-like 2 (NFE2L2) also act as a repressor of gene expression (Bahn *et al.*, 2019; Liu *et al.*, 2018; Thangasamy *et al.*, 2011; Timme-Laragy *et al.*, 2012). The expression of these

transcripts was upregulated in response to PCB126 exposure. It remains to be determined how increased methylation affects expression of these transcripts. Previous studies have shown that m6A methylation affects mRNA splicing. For instance, knockout of m6A writers and/or eraser proteins affects alternative splicing (AS) patterns (Dominissini *et al.*, 2012; Ping *et al.*, 2014; Zhao *et al.*, 2014; Zheng *et al.*, 2013). Similarly, m6A reader proteins recruited to m6A-modified transcripts are also shown to cause AS events by recruiting splicing factors (Kasowitz *et al.*, 2018). However, differential exon usage analysis did not reveal AS events among the differentially methylated transcripts. A recent study using exon arrays demonstrated that a potent AHR agonist, 2,3,7,8-tetrachlorodibenzo-*p*-dioxin (TCDD) induces AS in *ahrr* and *tiparp* transcripts in rodent livers (Villasenor-Altamirano *et al.*, 2019). Whether these AS events are due to m6A RNA methylation remains to be determined. Similarly, further characterization of post-transcriptional regulation of AHR target genes in zebrafish embryos is necessary to determine the effect of m6A RNA methylation on AS during periods of cellular differentiation.

In addition to AHR signaling, PCB126 exposure hypermethylated a few other coding and noncoding transcripts. Interestingly some of these transcripts were previously shown to be associated with AHR signaling. One of these is *plekhh3*, whose expression is inducible by AHR agonists in zebrafish and in mammals (Fracchiolla *et al.*, 2011; Frericks *et al.*, 2006). Another related hypermethylated transcript was *plekhg4b*, with unknown function. Pleckstrin homology domains are present in a variety of modular proteins involved in cellular signaling, cytoskeletal organization, membrane trafficking, and phospholipid processing (Scheffzek and Welti, 2012). Even though the role of *plekhh3* in AHR-induced signaling has not been characterized, biochemical mechanisms that mediate cellular toxicity by causing cytoskeleton disruption have been demonstrated. We also observed hypermethylation of *rpgra* transcripts, which are primarily localized to microtubules. Studies in mammals have demonstrated complex AS patterns of the RPGR gene, with over 20 splice variants (Ferreira, 2005; He *et al.*, 2008). It is possible that AS is regulated by m6A RNA methylation. Mutations in *rpgra* are associated with atrophic macular degeneration and primary cilia dyskinesia (Bukowy-Bieryllo *et al.*, 2013; Mawatari *et al.*, 2019) and splicing mutations in AHR have been associated with the development of retinitis pigmentosa (Zhou *et al.*, 2018). These results suggest that transcripts associated with AHR signaling are regulated by the m6A RNA modifications. Interestingly, the expression of *plekhh3* and *plekh4gb* is upregulated in response to PCB126 exposure. Further studies are needed to demonstrate the role of the epitranscriptome in xenobiotic and physiological functions of AHR.

We also observed three transcripts that lost methylation marks in response to PCB126 exposure, which are related to the nervous system (Balamurugan and Sterneck, 2013; Lewis *et al.*, 2015). For instance, *vgf*, a highly conserved neuroendocrine factor expressed exclusively in neuronal and neuroendocrine cells and induced by various growth factors (nerve growth factor, brain-derived neurotrophic factor and glial-derived growth factor) was hypomethylated in response to PCB126 exposure. VGF mRNA levels are regulated by neuronal activity, including long-term potentiation, seizure, and injury (Lewis *et al.*, 2015). Similarly, the *cebpd* gene encoding the C/EBPδ protein, a member of the C/EBP transcription factor family (Balamurugan and Sterneck, 2013) that modulates many biological processes including cell differentiation, proliferation, and cell death, was hypomethylated. Concomitantly, *vgf* and *cebpd* expression was also downregulated. In addition, an extracellular matrix family member, *sned1* (Leimeister *et al.*, 2004), an important player in embryogenesis particularly neurodevelopment was hypomethylated. These results are not surprising given the fact that dioxin-like PCBs have been shown to affect the nervous system (Aluru *et al.*, 2017; Glazer *et al.*, 2016; Orito *et al.*, 2007; Piedrafita *et al.*, 2008). Several recent studies have shown that m6A RNA modifications play an essential role in nervous system development (Livneh *et al.*, 2020; Xu *et al.*, 2020; Yu *et al.*, 2020). Further studies are needed to determine the role of mRNA m6A methylation in dioxin-like PCB effects on brain development, learning and memory, and other nervous system processes.

Our results led us to hypothesize that toxicant-induced alterations in m6A levels regulate the expression of transcripts by affecting mRNA stability. This is based on the observation that out of the 15 differentially methylated transcripts, 8 of them were found to be differentially expressed. Biochemical characterization studies have demonstrated that m6A is selectively recognized by binding proteins such as YTH domain family proteins and regulate mRNA stability (Wang *et al.*, 2014). It remains to be determined if toxicant-induced changes in gene expression are under epitranscriptomic regulation.

CONCLUSIONS

Here, we describe the first *in vivo* evidence demonstrating the effect of exposure to environmental chemicals on m6A RNA methylation landscape during vertebrate development. Our results indicate that regulation of m6A RNA methylation levels is one of the mechanisms by which PCB126 alters gene expression patterns. Further studies including time-course and dose-response are necessary to uncover the role of AHR in the regulation and biological functions of m6A during zebrafish development. In addition, characterization of the role of m6A RNA methylation in toxicant-induced phenotypes will provide a better understanding of the range of pathologies and diseases associated with environmental chemical exposures (Yang, 2020). Ever since the development of the MeRIP approach, substantial progress has been made in profiling m6A RNA modifications in a number of model systems. However, considerable limitations exist in quantitative determination of m6A patterns (McIntyre *et al.*, 2020). Recent methodological developments have overcome some of these hurdles and hence paving the way for better understanding of this important layer of gene regulation (Linder *et al.*, 2015; Meyer, 2019; Zhang *et al.*, 2019).

SUPPLEMENTARY DATA

Supplementary data are available at *Toxicological Sciences* online.

ACKNOWLEDGMENT

The authors would like to thank the toxicology lab group members at WHOI for their suggestions with data interpretation.

FUNDING

National Institute of Health National Institute of Environmental Health Sciences Outstanding New Environmental Scientist (NIH R01ES024915 to N.A.); Woods Hole Center for Oceans and Human Health [National

Institutes of Health (NIH) (Grant P01ES028938); National Science Foundation (Grant OCE-1840381) to M. E. Hahn, J. J. Stegeman, N.A., and S.K.].

DECLARATION OF CONFLICTING INTERESTS

The authors declared no potential conflicts of interest with respect to the research, authorship, and/or publication of this article.

REFERENCES

Aluru, N., and Karchner, S. I. (2020). PCB126 exposure revealed alterations in m6A RNA modifications in transcripts associated with AHR activation. Dryad, Dataset. Available at: https://doi.org/10.5061/dryad.h18931zj8. Accessed July 2020.

Aluru, N., Karchner, S. I., and Glazer, L. (2017). Early life exposure to low levels of AHR agonist PCB126 (3,3',4,4',5-pentachlorobiphenyl) reprograms gene expression in adult brain. *Toxicol. Sci.* **160**, 386–397.

Anders, S., Pyl, P. T., and Huber, W. (2015). HTSeq—A Python framework to work with high-throughput sequencing data. *Bioinformatics* **31**, 166–169.

Anders, S., Reyes, A., and Huber, W. (2012). Detecting differential usage of exons from RNA-seq data. *Genome Res.* **22**, 2008–2017.

Bahn, G., Park, J. S., Yun, U. J., Lee, Y. J., Choi, Y., Park, J. S., Baek, S. H., Choi, B. Y., Cho, Y. S., Kim, H. K., *et al.* (2019). NRF2/ARE pathway negatively regulates BACE1 expression and ameliorates cognitive deficits in mouse Alzheimer's models. *Proc. Natl. Acad. Sci. USA* **116**, 12516–12523.

Bai, L., Tang, Q., Zou, Z., Meng, P., Tu, B., Xia, Y., Cheng, S., Zhang, L., Yang, K., Mu, S., *et al.* (2018). m6A demethylase FTO regulates dopaminergic neurotransmission deficits caused by arsenite. *Toxicol. Sci.* **165**, 431–446.

Bailey, T. L., and Machanick, P. (2012). Inferring direct DNA binding from ChIP-seq. *Nucleic Acids Res.* **40**, e128.

Bailey, T. L., Boden, M., Buske, F. A., Frith, M., Grant, C. E., Clementi, L., Ren, J., Li, W. W., and Noble, W. S. (2009). MEME SUITE: Tools for motif discovery and searching. *Nucleic Acids Res.* **37**, W202–W208.

Balamurugan, K., and Sterneck, E. (2013). The many faces of C/EBPdelta and their relevance for inflammation and cancer. *Int. J. Biol. Sci.* **9**, 917–933.

Batista, P. J., Molinie, B., Wang, J., Qu, K., Zhang, J., Li, L., Bouley, D. M., Lujan, E., Haddad, B., Daneshvar, K., *et al.* (2014). m(6)A RNA modification controls cell fate transition in mammalian embryonic stem cells. *Cell Stem Cell* **15**, 707–719.

Behl, M., Ryan, K., Hsieh, J.-H., Parham, F., Shapiro, A. J., Collins, B. J., Sipes, N. S., Birnbaum, L. S., Bucher, J. R., Foster, P. M. D., *et al.* (2019). Screening for developmental neurotoxicity at the national toxicology program: The future is here. *Toxicol. Sci.* **167**, 6–14.

Bradford, Y. M., Toro, S., Ramachandran, S., Ruzicka, L., Howe, D. G., Eagle, A., Kalita, P., Martin, R., Taylor Moxon, S. A., Schaper, K., *et al.*. (2017). Zebrafish Models of Human Disease: Gaining Insight into Human Disease at ZFIN. *ILAR. J.* **58**, 4–16.

Bukowy-Bieryllo, Z., Zietkiewicz, E., Loges, N. T., Wittmer, M., Geremek, M., Olbrich, H., Fliegauf, M., Voelkel, K., Rutkiewicz, E., Rutland, J., *et al.* (2013). RPGR mutations might cause reduced orientation of respiratory cilia. *Pediatr. Pulmonol.* **48**, 352–363.

Cayir, A., Barrow, T. M., Guo, L., and Byun, H. M. (2019). Exposure to environmental toxicants reduces global N6-methyladenosine RNA methylation and alters expression of RNA methylation modulator genes. *Environ. Res.* **175**, 228–234.

Cayir, A., Byun, H.-M., and Barrow, T. M. (2020). Environmental epitranscriptomics. *Environ. Res.* **189**, 109885.

Chen, H., Zhao, T., Sun, D., Wu, M., and Zhang, Z. (2019). Changes of RNA N(6)-methyladenosine in the hormesis effect induced by arsenite on human keratinocyte cells. *Toxicol. In Vitro* **56**, 84–92.

Chen, J., Zhou, X., Wu, W., Wang, X., and Wang, Y. (2015). FTO-dependent function of N6-methyladenosine is involved in the hepatoprotective effects of betaine on adolescent mice. *J. Physiol. Biochem.* **71**, 405–413.

Coots, R. A., Liu, X. M., Mao, Y., Dong, L., Zhou, J., Wan, J., Zhang, X., and Qian, S. B. (2017). m(6)A facilitates eIF4F-independent mRNA translation. *Mol. Cell* **68**, 504–514 e7.

Desrosiers, R., Friderici, K., and Rottman, F. (1974). Identification of methylated nucleosides in messenger RNA from Novikoff hepatoma cells. *Proc. Natl. Acad. Sci. USA* **71**, 3971–3975.

Dobin, A., Davis, C. A., Schlesinger, F., Drenkow, J., Zaleski, C., Jha, S., Batut, P., Chaisson, M., and Gingeras, T. R. (2013). STAR: Ultrafast universal RNA-seq aligner. *Bioinformatics* **29**, 15–21.

Dominissini, D., Moshitch-Moshkovitz, S., Salmon-Divon, M., Amariglio, N., and Rechavi, G. (2013). Transcriptome-wide mapping of N(6)-methyladenosine by m(6)A-seq based on immunocapturing and massively parallel sequencing. *Nat. Protoc.* **8**, 176–189.

Dominissini, D., Moshitch-Moshkovitz, S., Schwartz, S., Salmon-Divon, M., Ungar, L., Osenberg, S., Cesarkas, K., Jacob-Hirsch, J., Amariglio, N., Kupiec, M., *et al.* (2012). Topology of the human and mouse m6A RNA methylomes revealed by m6A-seq. *Nature* **485**, 201–206.

Du, H., Zhao, Y., He, J., Zhang, Y., Xi, H., Liu, M., Ma, J., and Wu, L. (2016). YTHDF2 destabilizes m(6)A-containing RNA through direct recruitment of the CCR4-NOT deadenylase complex. *Nat. Commun.* **7**, 12626.

Engel, M., Eggert, C., Kaplick, P. M., Eder, M., Roh, S., Tietze, L., Namendorf, C., Arloth, J., Weber, P., Rex-Haffner, M., *et al.* (2018). The role of m(6)A/m-RNA methylation in stress response regulation. *Neuron* **99**, 389–403 e9.

Faroon, O., and Ruiz, P. (2016). Polychlorinated biphenyls: New evidence from the last decade. *Toxicol. Ind. Health* **32**, 1825–1847.

Ferreira, P. A. (2005). Insights into X-linked retinitis pigmentosa type 3, allied diseases and underlying pathomechanisms. *Hum. Mol. Genet.* **14**, R259–R267.

Fischer, J., Koch, L., Emmerling, C., Vierkotten, J., Peters, T., Bruning, J. C., and Ruther, U. (2009). Inactivation of the Fto gene protects from obesity. *Nature* **458**, 894–898.

Fracchiolla, N. S., Todoerti, K., Bertazzi, P. A., Servida, F., Corradini, P., Carniti, C., Colombi, A., Cecilia Pesatori, A., Neri, A., and Deliliers, G. L. (2011). Dioxin exposure of human CD34+ hemopoietic cells induces gene expression modulation that recapitulates its in vivo clinical and biological effects. *Toxicology* **283**, 18–23.

Frericks, M., Temchura, V. V., Majora, M., Stutte, S., and Esser, C. (2006). Transcriptional signatures of immune cells in aryl hydrocarbon receptor (AHR)-proficient and AHR-deficient mice. *Biol. Chem.* **387**, 1219–1226.

Galardi, S., Michienzi, A., and Ciafrè, S. A. (2020). Insights into the regulatory role of m(6)A epitranscriptome in glioblastoma. *Int. J. Mol. Sci.* **21, 2816**.

Geula, S., Moshitch-Moshkovitz, S., Dominissini, D., Mansour, A. A., Kol, N., Salmon-Divon, M., Hershkovitz, V., Peer, E., Mor, N., Manor, Y. S., *et al.* (2015). Stem cells. m6A mRNA methylation facilitates resolution of naive pluripotency toward differentiation. *Science* **347**, 1002–1006.

Glazer, L., Hahn, M. E., and Aluru, N. (2016). Delayed effects of developmental exposure to low levels of the aryl hydrocarbon receptor agonist 3,3',4,4',5-pentachlorobiphenyl (PCB126) on adult zebrafish behavior. *Neurotoxicology* **52**, 134–143.

Grunwald, D. J., and Eisen, J. S. (2002). Headwaters of the zebrafish — emergence of a new model vertebrate. *Nat. Rev. Genet.* **3**, 717–724.

Gu, S., Sun, D., Dai, H., and Zhang, Z. (2018). N(6)-methyladenosine mediates the cellular proliferation and apoptosis via microRNAs in arsenite-transformed cells. *Toxicol. Lett.* **292**, 1–11.

He, L., Li, H., Wu, A., Peng, Y., Shu, G., and Yin, G. (2019). Functions of N6-methyladenosine and its role in cancer. *Mol. Cancer* **18**, 176.

He, S., Parapuram, S. K., Hurd, T. W., Behnam, B., Margolis, B., Swaroop, A., and Khanna, H. (2008). Retinitis pigmentosa GTPase regulator (RPGR) protein isoforms in mammalian retina: Insights into X-linked retinitis pigmentosa and associated ciliopathies. *Vision Res.* **48**, 366–376.

Heck, A. M., and Wilusz, C. J. (2019). Small changes, big implications: The impact of m(6)A RNA methylation on gene expression in pluripotency and development. *Biochim. Biophys. Acta Gene Regul. Mech.* **1862**, 194402.

Huang, H., Weng, H., Sun, W., Qin, X., Shi, H., Wu, H., Zhao, B. S., Mesquita, A., Liu, C., Yuan, C. L., *et al.* (2018). Recognition of RNA N(6)-methyladenosine by IGF2BP proteins enhances mRNA stability and translation. *Nat. Cell Biol.* **20**, 285–295.

Ivanova, I., Much, C., Di Giacomo, M., Azzi, C., Morgan, M., Moreira, P. N., Monahan, J., Carrieri, C., Enright, A. J., and O'Carroll, D. (2017). The RNA m(6)A reader YTHDF2 is essential for the post-transcriptional regulation of the maternal transcriptome and oocyte competence. *Mol. Cell* **67**, 1059–1067 e4.

Jia, G., Fu, Y., Zhao, X., Dai, Q., Zheng, G., Yang, Y., Yi, C., Lindahl, T., Pan, T., Yang, Y. G., *et al.* (2011). N6-methyladenosine in nuclear RNA is a major substrate of the obesity-associated FTO. *Nat. Chem. Biol.* **7**, 885–887.

Jonsson, M. E., Kubota, A., Timme-Laragy, A. R., Woodin, B., and Stegeman, J. J. (2012). Ahr2-dependence of PCB126 effects on the swim bladder in relation to expression of CYP1 and cox-2 genes in developing zebrafish. *Toxicol. Appl. Pharmacol.* **265**, 166–174.

Kasowitz, S. D., Ma, J., Anderson, S. J., Leu, N. A., Xu, Y., Gregory, B. D., Schultz, R. M., and Wang, P. J. (2018). Nuclear m6A reader YTHDC1 regulates alternative polyadenylation and splicing during mouse oocyte development. *PLoS Genet.* **14**, e1007412.

Ke, S., Pandya-Jones, A., Saito, Y., Fak, J. J., Vågbø, C. B., Geula, S., Hanna, J. H., Black, D. L., Darnell, J. E. Jr., ., and Darnell, R. B. (2017). m(6)A mRNA modifications are deposited in nascent pre-mRNA and are not required for splicing but do specify cytoplasmic turnover. *Genes Dev.* **31**, 990–1006.

Leimeister, C., Schumacher, N., Diez, H., and Gessler, M. (2004). Cloning and expression analysis of the mouse stroma marker Snep encoding a novel nidogen domain protein. *Dev. Dyn.* **230**, 371–377.

Lewis, J. E., Brameld, J. M., and Jethwa, P. H. (2015). Neuroendocrine Role for VGF. *Front. Endocrinol.* **6**, 3.

Li, J., Yang, X., Qi, Z., Sang, Y., Liu, Y., Xu, B., Liu, W., Xu, Z., and Deng, Y. (2019). The role of mRNA m(6)A methylation in the nervous system. *Cell Biosci.* **9**, 66.

Linder, B., Grozhik, A. V., Olarerin-George, A. O., Meydan, C., Mason, C. E., and Jaffrey, S. R. (2015). Single-nucleotide-resolution mapping of m6A and m6Am throughout the transcriptome. *Nat. Methods* **12**, 767–772.

Liu, P., de la Vega, R., Sammani, M., Mascarenhas, S., Kerins, J. B., Dodson, M., Sun, M., Wang, X., Ooi, T., Garcia, A., *et al.* (2018). RPA1 binding to NRF2 switches ARE-dependent transcriptional activation to ARE-NRE-dependent repression. *Proc. Natl. Acad. Sci. USA* **115**, E10352–E10361.

Livneh, I., Moshitch-Moshkovitz, S., Amariglio, N., Rechavi, G., and Dominissini, D. (2020). The m(6)A epitranscriptome: Transcriptome plasticity in brain development and function. *Nat. Rev. Neurosci.* **21**, 36–51.

MacPherson, L., Ahmed, S., Tamblyn, L., Krutmann, J., Forster, I., Weighardt, H., and Matthews, J. (2014). Aryl hydrocarbon receptor repressor and TiPARP (ARTD14) use similar, but also distinct mechanisms to repress aryl hydrocarbon receptor signaling. *Int. J. Mol. Sci.* **15**, 7939–7957.

Mauer, J., and Jaffrey, S. R. (2018). FTO, m(6) Am, and the hypothesis of reversible epitranscriptomic mRNA modifications. *FEBS Lett.* **592**, 2012–2022.

Mawatari, G., Fujinami, K., Liu, X., Yang, L., Yokokawa, Y. F., Komori, S., Ueno, S., Terasaki, H., Katagiri, S., Hayashi, T., *et al.* (2019). Clinical and genetic characteristics of 14 patients from 13 Japanese families with RPGR-associated retinal disorder: Report of eight novel variants. *Hum. Genome Var.* **6**, 34.

McIntyre, A. B. R., Gokhale, N. S., Cerchietti, L., Jaffrey, S. R., Horner, S. M., and Mason, C. E. (2020). Limits in the detection of m(6)A changes using MeRIP/m(6)A-seq. *Sci. Rep.* **10**, 6590.

Meyer, K. D. (2019). DART-seq: an antibody-free method for global m6A detection. *Nat. Methods.* **16**, 1275–1280.

Meyer, K. D., and Jaffrey, S. R. (2017). Rethinking m(6)A readers, writers, and erasers. *Annu. Rev. Cell Dev. Biol.* **33**, 319–342.

Meyer, K. D., Saletore, Y., Zumbo, P., Elemento, O., Mason, C. E., and Jaffrey, S. R. (2012). Comprehensive analysis of mRNA methylation reveals enrichment in 3' UTRs and near stop codons. *Cell* **149**, 1635–1646.

Nacci, D. E., Champlin, D., and Jayaraman, S. (2010). Adaptation of the estuarine fish fundulus heteroclitus (Atlantic Killifish) to polychlorinated biphenyls (PCBs). *Estuaries Coasts* **33**, 853–864.

Nishimura, Y., Inoue, A., Sasagawa, S., Koiwa, J., Kawaguchi, K., Kawase, R., Maruyama, T., Kim, S., and Tanaka, T. (2016). Using zebrafish in systems toxicology for developmental toxicity testing. *Congenit Anom (Kyoto)*. **56**, 18–27.

Orito, K., Gotanda, N., Murakami, M., Ikeda, T., Egashira, N., Mishima, K., and Fujiwara, M. (2007). Prenatal exposure to 3,3',4,4',5-pentachlorobiphenyl (PCB126) promotes anxiogenic behavior in rats. *Tohoku J. Exp. Med.* **212**, 151–157.

Piedrafita, B., Erceg, S., Cauli, O., Monfort, P., and Felipo, V. (2008). Developmental exposure to polychlorinated biphenyls PCB153 or PCB126 impairs learning ability in young but not in adult rats. *Eur. J. Neurosci.* **27**, 177–182.

Ping, X. L., Sun, B. F., Wang, L., Xiao, W., Yang, X., Wang, W. J., Adhikari, S., Shi, Y., Lv, Y., Chen, Y. S., *et al.* (2014). Mammalian WTAP is a regulatory subunit of the RNA N6-methyladenosine methyltransferase. *Cell Res.* **24**, 177–189.

Robinson, M. D., McCarthy, D. J., and Smyth, G. K. (2010). edgeR: A Bioconductor package for differential expression analysis of digital gene expression data. *Bioinformatics* **26**, 139–140.

Roundtree, I. A., Luo, G. Z., Zhang, Z., Wang, X., Zhou, T., Cui, Y., Sha, J., Huang, X., Guerrero, L., Xie, P., *et al.* (2017). YTHDC1 mediates nuclear export of N(6)-methyladenosine methylated mRNAs. *Elife* **6**.

Scheffzek, K., and Welti, S. (2012). Pleckstrin homology (PH) like domains - versatile modules in protein-protein interaction platforms. *FEBS Lett.* **586**, 2662–2673.

Schwartz, S., Mumbach, M. R., Jovanovic, M., Wang, T., Maciag, K., Bushkin, G. G., Mertins, P., Ter-Ovanesyan, D., Habib, N., Cacchiarelli, D., *et al.* (2014). Perturbation of m6A writers reveals two distinct classes of mRNA methylation at internal and 5' sites. *Cell Rep.* **8**, 284–296.

Shi, H., Wang, X., Lu, Z., Zhao, B. S., Ma, H., Hsu, P. J., Liu, C., and He, C. (2017). YTHDF3 facilitates translation and decay of N(6)-methyladenosine-modified RNA. *Cell Res.* **27**, 315–328.

Smedley, D., Haider, S., Durinck, S., Pandini, L., Provero, P., Allen, J., Arnaiz, O., Awedh, M. H., Baldock, R., Barbiera, G., *et al.* (2015). The BioMart community portal: An innovative alternative to large, centralized data repositories. *Nucleic Acids Res.* **43**, W589–98.

Stark, R., and Brown, G. (2011). DiffBind: Differential binding analysis of ChIP-Seq peak data. Available at: http://bioconductor.org/packages/release/bioc/vignettes/DiffBind/inst/doc/DiffBind.pdf. Accessed July 2020.

Tang, C., Klukovich, R., Peng, H., Wang, Z., Yu, T., Zhang, Y., Zheng, H., Klungland, A., and Yan, W. (2018). ALKBH5-dependent m6A demethylation controls splicing and stability of long 3'-UTR mRNAs in male germ cells. *Proc. Natl. Acad. Sci. USA* **115**, E325–E333.

Thangasamy, A., Rogge, J., Krishnegowda, N. K., Freeman, J. W., and Ammanamanchi, S. (2011). Novel function of transcription factor Nrf2 as an inhibitor of RON tyrosine kinase receptor-mediated cancer cell invasion. *J. Biol. Chem.* **286**, 32115–32122.

Timme-Laragy, A. R., Karchner, S. I., Franks, D. G., Jenny, M. J., Harbeitner, R. C., Goldstone, J. V., McArthur, A. G., and Hahn, M. E. (2012). Nrf2b, novel zebrafish paralog of oxidant-responsive transcription factor NF-E2-related factor 2 (NRF2). *J. Biol. Chem.* **287**, 4609–4627.

Villasenor-Altamirano, A. B., Watson, J. D., Prokopec, S. D., Yao, C. Q., Boutros, P. C., Pohjanvirta, R., Valdes-Flores, J., and Elizondo, G. (2019). 2,3,7,8-Tetrachlorodibenzo-p-dioxin modifies alternative splicing in mouse liver. *PLoS One* **14**, e0219747.

Vu, L. P., Cheng, Y., and Kharas, M. G. (2019). The biology of m(6)A RNA methylation in normal and malignant hematopoiesis. *Cancer Discov.* **9**, 25–33.

Wang, X., Lu, Z., Gomez, A., Hon, G. C., Yue, Y., Han, D., Fu, Y., Parisien, M., Dai, Q., Jia, G., *et al.* (2014). N6-methyladenosine-dependent regulation of messenger RNA stability. *Nature* **505**, 117–120.

Wang, X., Zhao, B. S., Roundtree, I. A., Lu, Z., Han, D., Ma, H., Weng, X., Chen, K., Shi, H., and He, C. (2015). N(6)-methyladenosine modulates messenger RNA translation efficiency. *Cell* **161**, 1388–1399.

Xiao, W., Adhikari, S., Dahal, U., Chen, Y. S., Hao, Y. J., Sun, B. F., Sun, H. Y., Li, A., Ping, X. L., Lai, W. Y., *et al.* (2016). Nuclear m(6)A reader YTHDC1 regulates mRNA splicing. *Mol. Cell* **61**, 507–519.

Xu, H., Dzhashiashvili, Y., Shah, A., Kunjamma, R. B., Weng, Y. L., Elbaz, B., Fei, Q., Jones, J. S., Li, Y. I., Zhuang, X., *et al.* (2020). m(6)A mRNA methylation is essential for oligodendrocyte maturation and CNS myelination. *Neuron* **105**, 293–309 e5.

Yang, C. (2020). ToxPoint: Dissecting functional RNA modifications in responses to environmental exposure-mechanistic toxicology research enters a New Era. *Toxicol. Sci.* **174**, 1–2.

Yang, E., Pavuk, M., Sjodin, A., Lewin, M., Jones, R., Olson, J., and Birnbaum, L. (2018). Exposure of dioxin-like chemicals in participants of the Anniston community health survey follow-up. *Sci. Total Environ.* **637–638**, 881–891.

Yu, J., Zhang, Y., Ma, H., Zeng, R., Liu, R., Wang, P., Jin, X., and Zhao, Y. (2020). Epitranscriptomic profiling of N6-methyladenosine-related RNA methylation in rat cerebral cortex following traumatic brain injury. *Mol. Brain* **13**, 11.

Zaccara, S., Ries, R. J., and Jaffrey, S. R. (2019). Reading, writing and erasing mRNA methylation. *Nat. Rev. Mol. Cell Biol.* **20**, 608–624.

Zeng, Y., Wang, S., Gao, S., Soares, F., Ahmed, M., Guo, H., Wang, M., Hua, J. T., Guan, J., Moran, M. F., *et al.* (2018). Refined RIP-seq protocol for epitranscriptome analysis with low input materials. *PLoS Biol.* **16**, e2006092.

Zhang, Z., Chen, L.-Q., Zhao, Y.-L., Yang, C.-G., Roundtree, I. A., Zhang, Z., Ren, J., Xie, W., He, C., and Luo, G.-Z. (2019). Single-base mapping of m 6 A by an antibody-independent method. *Sci. Adv.* **5**, eaax0250.

Zhang, C., Chen, Y., Sun, B., Wang, L., Yang, Y., Ma, D., Lv, J., Heng, J., Ding, Y., Xue, Y., *et al.* (2017). m(6)A modulates haematopoietic stem and progenitor cell specification. *Nature* **549**, 273–276.

Zhao, B. S., Wang, X., Beadell, A. V., Lu, Z., Shi, H., Kuuspalu, A., Ho, R. K., and He, C. (2017). m(6)A-dependent maternal mRNA clearance facilitates zebrafish maternal-to-zygotic transition. *Nature* **542**, 475–478.

Zhao, T., Li, X., Sun, D., and Zhang, Z. (2019). Oxidative stress: One potential factor for arsenite-induced increase of N(6)-methyladenosine in human keratinocytes. *Environ. Toxicol. Pharmacol.* **69**, 95–103.

Zhao, X., Yang, Y., Sun, B. F., Shi, Y., Yang, X., Xiao, W., Hao, Y. J., Ping, X. L., Chen, Y. S., Wang, W. J., *et al.* (2014). FTO-dependent demethylation of N6-methyladenosine regulates mRNA splicing and is required for adipogenesis. *Cell Res.* **24**, 1403–1419.

Zheng, G., Dahl, J. A., Niu, Y., Fedorcsak, P., Huang, C. M., Li, C. J., Vagbo, C. B., Shi, Y., Wang, W. L., Song, S. H., *et al.* (2013). ALKBH5 is a mammalian RNA demethylase that impacts RNA metabolism and mouse fertility. *Mol. Cell* **49**, 18–29.

Zhong, X., Yu, J., Frazier, K., Weng, X., Li, Y., Cham, C. M., Dolan, K., Zhu, X., Hubert, N., Tao, Y., *et al.* (2018). Circadian clock regulation of hepatic lipid metabolism by modulation of m(6)A mRNA methylation. *Cell Rep.* **25**, 1816–1828 e4.

Zhou, K. I., Shi, H., Lyu, R., Wylder, A. C., Matuszek, Z., Pan, J. N., He, C., Parisien, M., and Pan, T. (2019). Regulation of co-transcriptional pre-mRNA splicing by m(6)A through the low-complexity protein hnRNPG. *Mol. Cell* **76**, 70–81 e9.

Zhou, Y., Li, S., Huang, L., Yang, Y., Zhang, L., Yang, M., Liu, W., Ramasamy, K., Jiang, Z., Sundaresan, P., *et al.* (2018). A splicing mutation in aryl hydrocarbon receptor associated with retinitis pigmentosa. *Hum. Mol. Genet.* **27**, 2563–2572.